# Determination of the smoke-plume heights and their dynamics with ground-based scanning lidar

V. Kovalev,* A. Petkov, C. Wold, S. Urbanski, and W. M. Hao

Forest Service, U.S. Department of Agriculture, Fire Sciences Laboratory, 5775 Hwy 10 West, Missoula, Montana 59808, USA

*Corresponding author: vladimirakovalev@fs.fed.us

Lidar-data processing techniques are analyzed, which allow determining smoke-plume heights and their dynamics and can be helpful for the improvement of smoke dispersion and air quality models. The data processing algorithms considered in the paper are based on the analysis of two alternative characteristics related to the smoke dispersion process: the regularized intercept function, extracted directly from the recorded lidar signal, and the square-range corrected backscatter signal, obtained after determining and subtracting the constant offset in the recorded signal. The analysis is performed using experimental data of the scanning lidar obtained in the area of prescribed fires.   © 2015 Optical Society of America

*OCIS codes:*   (280.1100) Aerosol detection; (280.1120) Air pollution monitoring; (290.1090) Aerosol and cloud effects.

http://dx.doi.org/10.1364/AO.54.002011

## 1.   Introduction

Wildland fires can have negative impacts on human health by contributing to unhealthy levels of aerosol particle content. The smoke obscuration of roadways and airport runways and reduced visibility is another adverse impact from wildfires. The EPA's reduction of the ambient PM2.5 standard for 24 h has significantly increased the regulatory demands for land management agencies to address the air quality impact of wildland-fire emissions. To comply with the regulatory rules, land management needs the opportunity to predict the possible effects of wildfires and levels of contribution of fire emissions to atmospheric pollution. However, current smoke-dispersion models do not allow reliable estimation of the local and regional impacts of the fire's smoke emissions. The uncertainties and biases of these models and the corresponding limits of their applications are poorly characterized.

Smoke dispersion in the atmosphere strongly depends on the height at which wildfire smoke particulates are injected into the atmosphere. In turn, the upper boundary of the plume height, which is a key input to aerosol transport models, depends on the heat release rate from the fire, the moisture content of the fuels, and the atmospheric conditions [1,2]. The proper characterization of this height is an issue. There are not enough experimental data about smoke plume rise and dynamics, pollutant concentrations, and smoke particulate transport from wildland fires to validate these models. The absence of such experimental data, such as the distribution of smoke particles, plume height, rise, dynamics, and dispersion, impedes the validation and improvement of the existing smoke-dispersion models.

Quantifying the plume heights under different meteorological conditions can potentially be achieved by the application of the remote sensing technique. Lidar profiling of the atmosphere is one of the most suitable methods for this purpose. It allows extracting vertical profiles of the smoke plumes and investigating smoke plume heights and downdrafts

that transport the smoke particulates downward, worsening air quality at ground level.

During the last decade, a number studies were published in which the characterization of smoke plume behavior, including estimates of the plume injection height, were made using the information derived from satellite data, in particular from the CALIPSO data [3–7]. However, the information derived from space data is limited to the smoke plumes having discernable features. The satellite measurements are most effective when wildfires produce plumes that penetrate through the boundary layer and are transported downwind over great distances. These satellite measurements are much less effective for the investigation of the smoke that remains within the boundary layer.

## 2. Smoke-Plume Height Measurement Methodology and Algorithms for Ground-Based Lidar

For investigation of the characteristics of the smoke plumes that remain within the boundary layer, ground-based lidar may be considered the best option. To determine the smoke-plume height with ground-based lidar, the latter should have scanning abilities both in the azimuthal and slope directions. A general schematic for determining the smoke plume height with scanning lidar is shown in Fig. 1. The lidar, located in the close vicinity of a local scale fire, scans the plume under a number of elevation angles. The slant lines in the figure show the directions of lidar scanning, and the filled dots show the maximum height of the smoke plume fixed under different elevation angles.

Let us consider examples of the real experimental data obtained on August 25, 2013, with the Missoula Fire Sciences Laboratory scanning lidar in the area of the prescribed fires near Walla Walla, Washington, USA. The elements of the mobile lidar used in this investigation are as follows [8]. A short-pulsed Nd:YAG laser attached to the top of a receiving telescope is used as the light source. The lidar receiver measures the backscatter signal at two wavelengt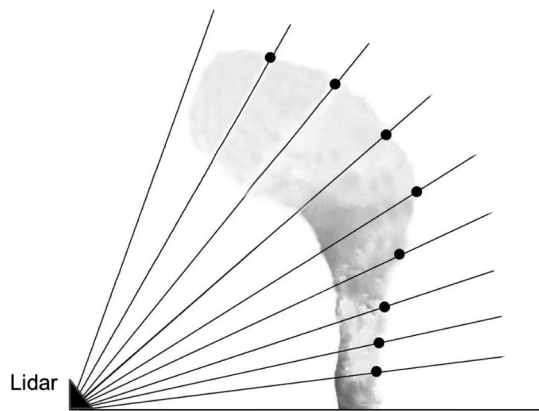hs, 532 and 1064 nm, simultaneously. The laser beam is emitted parallel to the telescope after going through a periscope, so that the effective exit aperture is offset 0.41 m from the center of the telescope. The periscope increases the distance at which the laser beam overlaps the telescope field of view up to ~1000 m, simultaneously decreasing the dynamic range of the signals and increasing the total measurement range. The telescope–laser system is able to turn through 180° horizontally and 90° vertically. In the experiment, the vertical scans were performed in a fixed azimuthal direction, and only the backscatter signals at 1064 nm were applied for the analysis. The vertical scans were made within the angular sector from 5° to 60° with an angle resolution of 1°. Each recorded signal was the average of 30 shots, and each total scan was recorded for ~75 s.

Different optical situations can be encountered when profiling smoke plumes with scanning lidar [8–11]. Many such situations were met when profiling the prescribed fires near Walla Walla. The typical optical situations met on August 25 are illustrated in Figs. 2(a)–2(d). Initially, when the prescribed fire is starting, the vertically stratified smoke-plume column without well-defined horizontal layering in its vicinity is observed [Fig. 2(a)]. Then the smoke plume aerosols start accumulating in the vicinity of the maximum height of the vertically stratified plume [Fig. 2(b)]. The strong dispersing processes create the specific combination in which the vertically stratified smoke plume and horizontal smoke-plume layering take place [Fig. 2(c)]. Finally, when the fuel for the fire becomes exhausted, the vertical smoke-plume structure degrades. At that stage, the smoke plume particles create a horizontal (or close to horizontal) layer elevated over ground level [Fig. 2(d)].

There is some inconsistency in the term "injection height" and little probability of its accurate determination, especially when using the satellite lidar. The plume injection height is commonly defined as the vertical zone in which a buoyant plume begins to transport horizontally away from its origin source [3]. Meanwhile, in many cases, the lidar can reliably determine only the top of such a zone. The bottom part of this zone is often extremely dispersed; moreover, it may have a multilayered structure or extend down to ground level, so that even the definition of the lowest boundary of the injection height is an issue. Meanwhile, just the top of this height determines the maximum distance over which the smoke plume may travel and impact its destination, for example, Arctic ice. Keeping this observation in mind, we will focus here on determining the maximum plume height when the smoke plume reveals well-developed horizontal layering, such as in Figs. 2(b)–2(d).

The use of alternative data processing techniques for determining the plume height dispersion may yield not only the main parameter of interest, the maximum smoke-plume height, but also some related smoke-plume characteristics. Let us start with the data processing technique of detecting dispersed



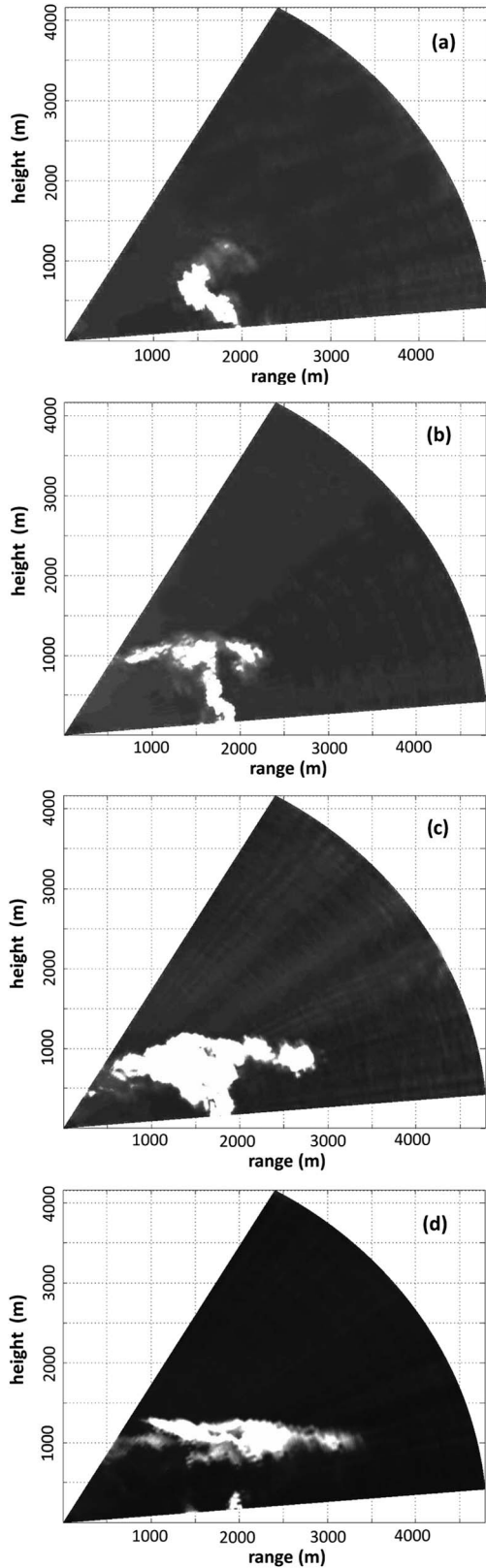Fig. 1. Schematic of determining the height of the smoke-plume column with scanning lidar.

Lidar

Fig. 2. (a) The white contour shows the two-dimensional image of the smoke-plume boundaries determined on August 25, 2013, at 10:57 local time; (b) same as in (a) but at 11:03; (c) same as in (a) but at 11:08; (d) same as in (a) but at 11:23.

smoke-plume layering and determining its maximum height, discussed in [12–15]. The total signal at the height $h$, measured in the slope direction, $\varphi$, is a sum of the backscatter signal, $P_\varphi(h)$, and a constant component, $B_\varphi$; that is, $P_{\varphi,\Sigma}(h) = P_\varphi(h) + B_\varphi$. For each slope direction and each discrete height, … $h_j - \Delta h$, $h_j$, $h_j + \Delta h$…, the auxiliary function,

$$Y_\varphi(h) = P_{\varphi,\Sigma}(h)x, \qquad (1)$$

is calculated; here $x = \frac{h^2}{(\sin \varphi)^2}$. Using principles similar to those in [12], the regularized intercept function, $Y_0(\varphi, x)$, for any slope direction $\varphi$ may be determined as

$$Y_0(\varphi, x) = \left| \frac{Y_{\varphi,x} - \frac{dY_{\varphi,x}}{dx}}{x + \Delta_\varphi} \right|; \qquad (2)$$

here $\Delta_\varphi$ is a user-defined positive nonzero constant, chosen within the range (0.02–0.05) from the maximum value of $x$ over the analyzed height interval. Note that before differentiation, the function $Y_\varphi(h)$ in Eq. (1) is transformed into a function of variable $x$ and denoted in Eq. (2) as $Y_{\varphi,x}$; after determining the intercept function, $Y_0(\varphi, x)$, it is transformed back to the function of height, $Y_0(\varphi, h)$. These functions are then used to determine the maximum heterogeneity function at each height, that is,

$$Y_{0,\max}(h) = \max[Y_0(\varphi_{\min}, h), …Y_0(\varphi_j, h),$$
$$Y_0(\varphi_{j+1}, h), …, Y_0(\varphi_{\max}, h)]. \qquad (3)$$

The above function is normalized to a unit that is determined as the ratio

$$Y_{0,\mathrm{norm}}(h) = \frac{Y_{0,\max}(h)}{Y_{0,\max,\max}}, \qquad (4)$$

where $Y_{0,\max,\max}$ is the maximum value of $Y_{0,\max}(h)$ within the angular sector scanned by the lidar.

The set of the functions, $Y_0(\varphi, h)$, determined for the lidar scans shown in Figs. 2(a)–2(d) and normalized to the unit, and the corresponding functions, $Y_{0,\mathrm{norm}}(h)$, are shown in Figs. 3(a)–3(d). The specific shape of these curves follows from Eq. (2); in particular, it depends on the derivative, $\frac{dY_{\varphi,x}}{dx}$. Accordingly, the variations in the functions $Y_{0,\mathrm{norm}}(h)$ are related to the boundaries of the areas of increased backscattering rather than to intensity of the backscattering and smoke-plume concentration. The areas where $Y_{0,\mathrm{norm}}(h) \to 1$ are the areas of the highest aerosol heterogeneity.

The simplest principle of determining the maximum plume height is selecting the appropriate fixed level $\chi < 1$ and determining the height at which $Y_{0,\mathrm{norm}}(h) = \chi$. The main issue in such a simple approach is the rational selection of the level $\chi$. In the case of a poorly defined boundary, as is generally the case in smoke-polluted atmospheres, the height,
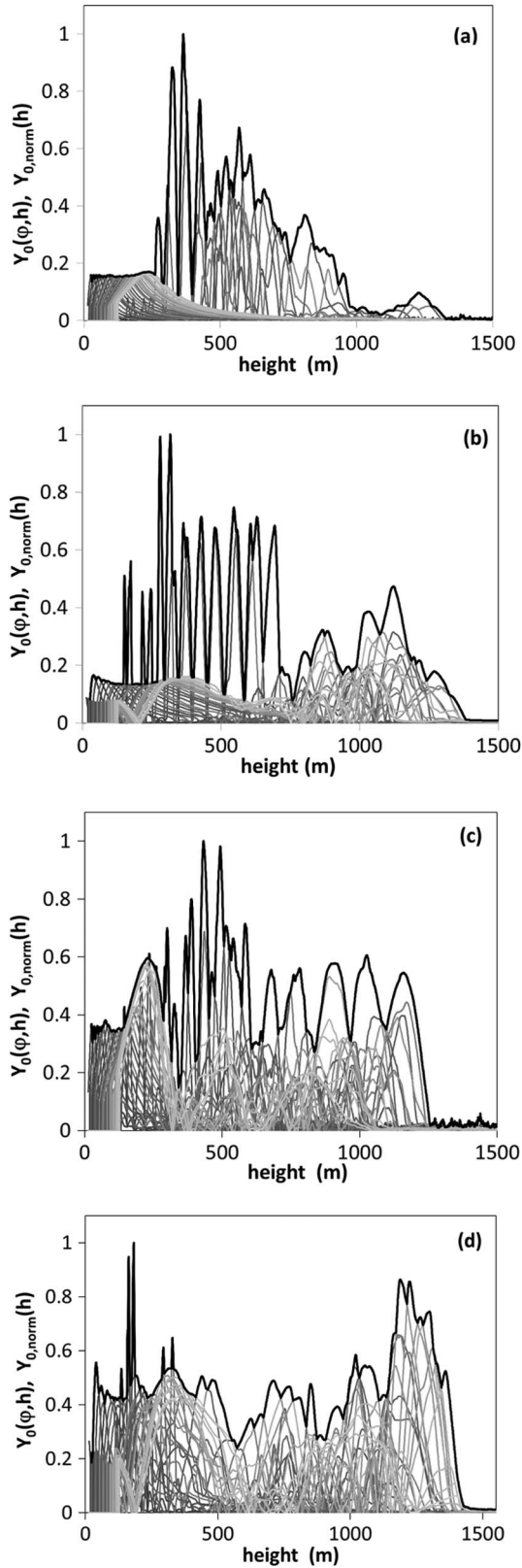
Fig. 3. (a)–(d) Thin solid curves represent the functions $Y_0(\varphi, h)$ determined from the scanning lidar signals at the same time periods as the scans shown in Figs. 2(a)–2(d), respectively; these functions, obtained from the signals at the wavelength 1064 nm, are normalized to unit. The corresponding functions, $Y_{0,\mathrm{norm}}(h)$, are shown as the black bold curves.

$h(\chi)$, at which the selected parameter, $\chi$, matches $Y_{0,\mathrm{norm}}(h)$ can dramatically depend on $\chi$ [3,13]. The most effective method for such data analysis is examining the changes in the height of the smoke-plume boundary when different $\chi$ are used. In Figs. 4(a)–4(d), the dependence of the heights $h(\chi)$ on different $\chi$ are shown for the same cases as in Figs. 3(a)–3(d). One can see that the well-defined boundary of the smoke plume can be observed only in Fig. 4(d), whereas in other cases the smoke plumes are significantly dispersed, having multilayer structures [Figs. 4(b) and 4(c)].

An alternative way of determining the upper boundary of the smoke plume may be based on the straightforward usage of the signals of scanning lidar. In this variant, the simplest function, the square-range-corrected signal, may be used as a basic function. The signal as the function of the slope $\varphi$ and the height, $h$, that is,

$$S(\varphi, h) = P_\varphi(h)(h/\sin \varphi)^2, \qquad (5)$$

is calculated with the straightforward formula,

$$S(\varphi, h) = [P_{\varphi,\Sigma}(h) - \langle B_\varphi \rangle](h/\sin \varphi)^2, \qquad (6)$$

where $\langle B_\varphi \rangle$ is the estimate of the constant component, $B_\varphi$, at the slope direction $\varphi$; it may be found using the same lidar signals, $P_{\varphi,\Sigma}(h)$, recorded over distant ranges where the backscatter signal presumably vanishes, that is, $P_\varphi(h) \approx 0$. The sets of the functions $S(\varphi, h)$ determined for the same lidar scans within the angular sector from $\varphi_{\min}$ to $\varphi_{\max}$ are shown in Figs. 5(a)–5(d).

To simplify determining the maximum plume heights of interest, the maximum function, $S_{\max}(h)$, should be transformed similar to the above function $Y_{0,\max}(h)$; that is, it should be calculated from the set of the functions, $S(\varphi, h)$, as

$$S_{\max}(h) = \max[S(\varphi_{\min}, h), \ldots S(\varphi_j, h),$$
$$S(\varphi_{j+1}, h), \ldots, S(\varphi_{\max}, h)], \qquad (7)$$

and then normalized to unit, that is,

$$S_{\mathrm{norm}}(h) = \frac{S_{\max}(h)}{S_{\max,\max}}; \qquad (8)$$

here $S_{\max,\max}$ is the maximum value of $S_{\max}(h)$ within the altitude range from $h_1 = r_{\min} \sin \varphi_{\min}$ to $h_2 = r_{\max} \sin \varphi_{\max}$, where $r_{\min}$ and $r_{\max}$ are bordering points of the lidar operative range. The range of the normalized function, $S_{\mathrm{norm}}(h)$, may vary from zero to unit, the same as the range of the function $Y_{0,\mathrm{norm}}(h)$. Generally, the functions $S(\varphi, h)$ are extremely scattered; therefore, in practice, it is sensible to average the initial function $S_{\max}(h)$ before determining $S_{\mathrm{norm}}(h)$.

The normalization of the square-range-corrected signal allows determining the smoke-plume maximum
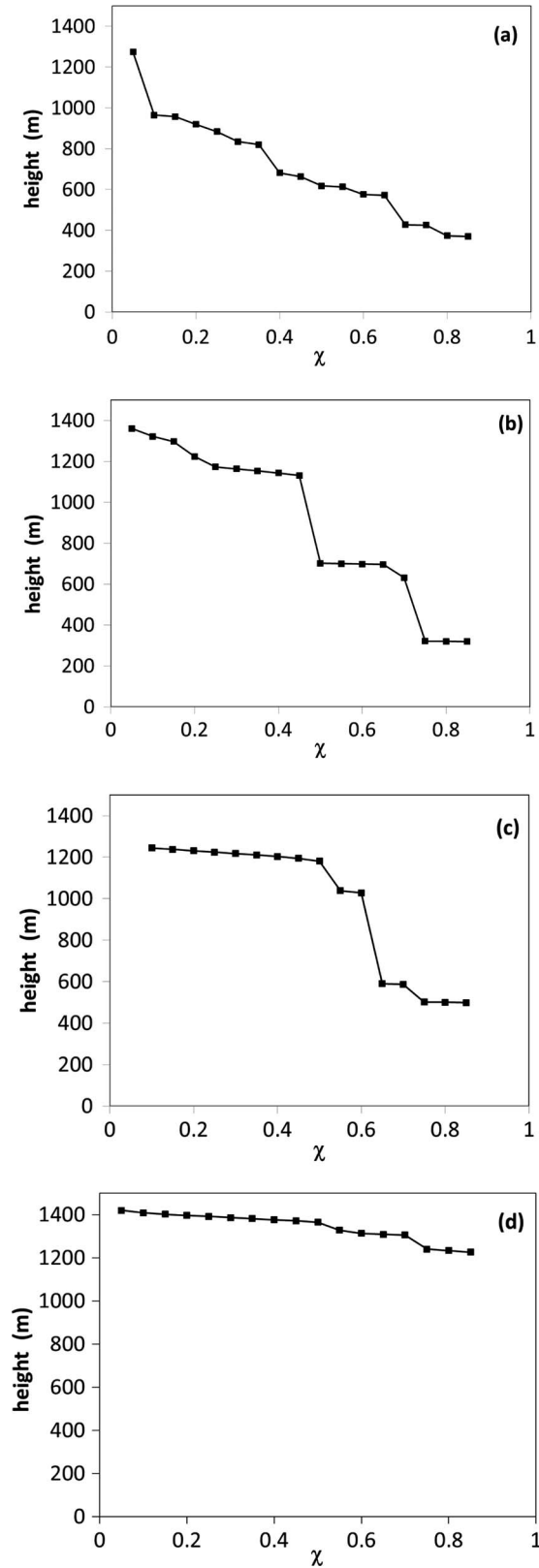
Fig. 4. (a)–(d) Dependence of the estimated height, $h(\chi)$, on the selected $\chi$ for the functions $Y_{0,\mathrm{norm}}(h)$ presented in Figs. 3(a)–3(d), respectively.
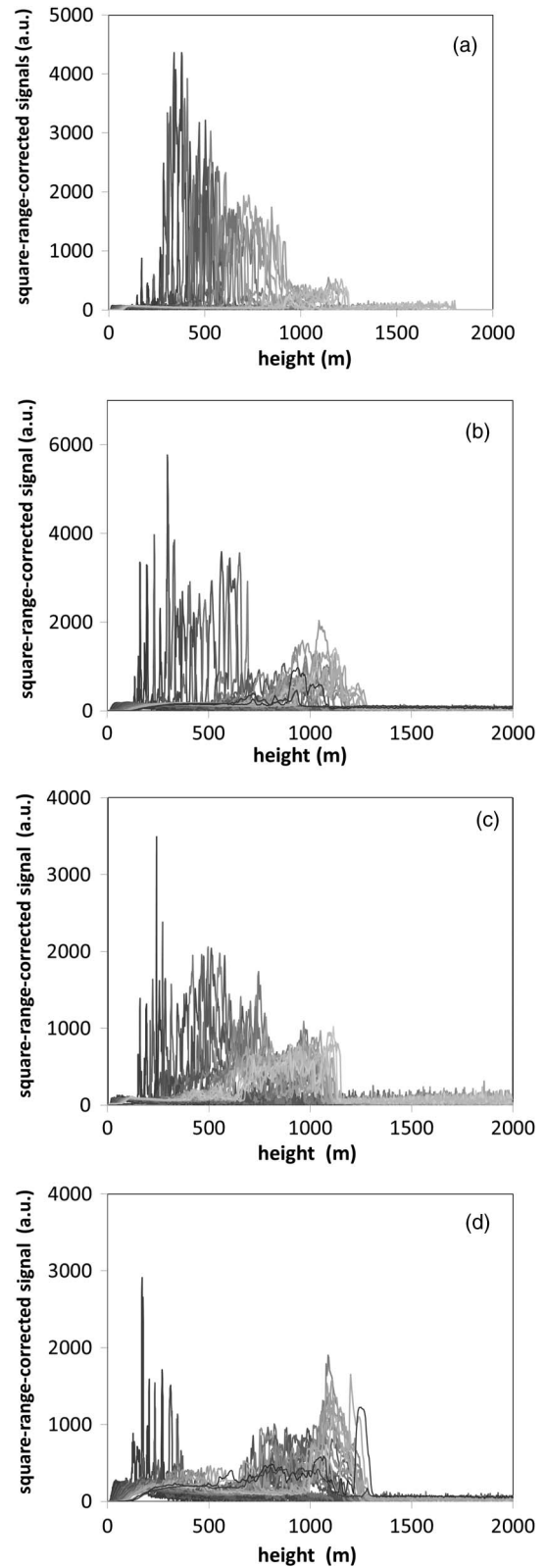


Fig. 5. (a)–(d) Square-range-corrected signals of the scanning lidar at the wavelength 1064 nm as a function of height for the lidar scans in Figs. 3(a)–3(d), respectively.
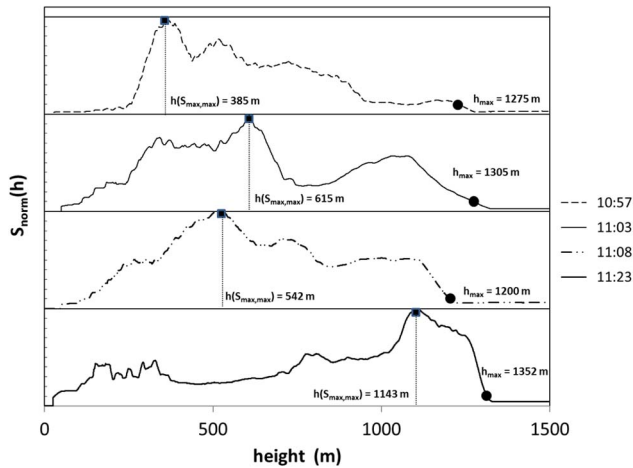
Fig. 6. Normalized functions, $S_{\text{norm}}(h)$, for the lidar scans under consideration. The heights, $h(S_{\text{max,max}})$, for the times shown in the legend are shown as filled squares. The filled dots show the maximum smoke-plume heights determined for the level $\chi = 0.1$.
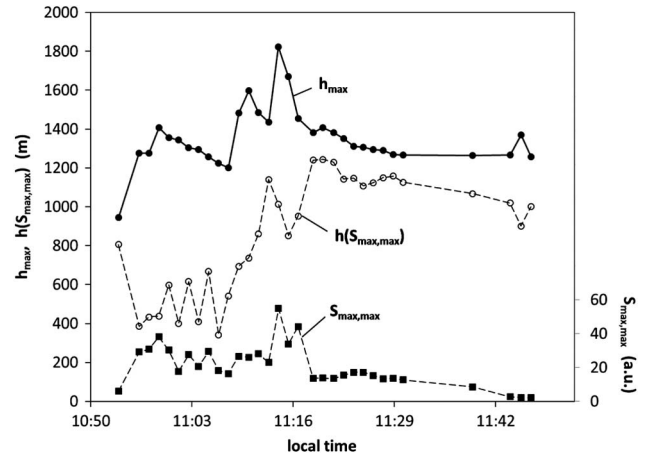


Fig. 7. Variations of the maximum values of the square-range-corrected signals, $S_{\text{max,max}}$; their heights, $h(S_{\text{max,max}})$; and the heights, $h_{\text{max}}$, determined at the level $\chi = 0.1$, during the time period from 10:57 to 11:47 on August 25, 2014.

height using the selected levels, $\chi < 1$, the same as was done above for the function $Y_{0,\text{norm}}(h)$. In Fig. 6, typical normalized functions, $S_{\text{norm}}(h)$, are shown. Here the filled circles show the smoke-plume maximum heights determined at the level $\chi = 0.1$, whereas the filled squares show the heights where $S_{\text{norm}}(h)$ reaches its maximum value equal to the unit.

As stated in [3], the surface smoke-particulate concentration, predicted by models, is sensitive to the amount of plume mass injected at various heights. Knowledge of the vertical structures of smoke plumes may allow better smoke-dispersion predictions. Assuming that the vertical structure of plume concentration and the shape of the lidar backscatter signal are related, the utilization of the normalized square-range-corrected signals versus height allows obtaining some information about the investigated smoke plumes. Such a method can provide experimental data that allow some estimation of the temporal variations of the smoke-plume concentration at different heights and the height at which the smoke-plume concentration presumably is at a maximum. As shown in Fig. 6, these heights, symbolized as $h(S_{\text{max,max}})$, increased from 385 to 1143 m during the period from 10:57 to 11:23.

The rate of heat release, which can be monitored by the behavior of the parameter $S_{\text{max,max}}$, is directly related to the rate of biomass consumption. In Fig. 7, the variations of the heights $h(S_{\text{max,max}})$, at which the maximum backscatter signals were located are shown during the whole period of smoke-plume profiling. One can see that initially, at 10:57, the most intensive smoke particulates were located in the vicinity of the height $h(S_{\text{max,max}}) \approx 400$ m; then the height increases, reaching its maximum, 1244 m, at 11:20. After that it decreases down to the heights 900–1000 m. The maximum backscattering intensity, $S_{\text{max,max}}$, equal to 54.9 a.u., was fixed at 11:14; then it monotonically decreased, vanishing at the end of the prescribed burn period, at 11:47.

Performing such an analysis, one should keep in mind that there is no simple relationship between the smoke-plume concentration and the backscatter signal obtained in the process of profiling the smoke plume. Nevertheless, two assumptions used in the above analysis look sensible; first, in not too dense smokes, the heights of the maximum smoke-plume concentration and the maximum backscatter signal are the same, or at least, are close to each other; second, the temporal variations of the maximum smoke-plume concentration and the maximum backscatter signal are similar. However, in some cases, these assumptions may be not met, and the vertical profiles of these parameters may be significantly different.

One more comment about the latter variant is required. The use of the shape of the square-range-corrected lidar signal for determining smoke-plume maximum height requires a preliminary estimate of the sensible maximum lidar range, $r_{\text{max}}$. The square-range-corrected signal over distant ranges is generally corrupted with extensive random noise, which may completely mask important specifics in the shape of the recorded backscatter signal and, accordingly, in the shape of the function $S_{\text{norm}}(h)$. To avoid this issue, a sensible maximum range for the signals needs to be established before these signals versus range are transformed into these versus height. In principle, this can be achieved by selecting some acceptable signal-to-noise ratio in the lidar signal. However, no standard method for selecting such a fixed signal-to-noise ratio level exists except methods based on pure statistical principles. Unfortunately, these principles may be not valid for our task, where the results depend on how well the smoke-plume boundary is defined. The simplest way of making such a selection is to vary the maximum height, starting it with approximately doubled distance from the lidar to smoke plume origin, then increasing it until large noise appears. In our study, the discrete changes of $r_{\text{max}}$ from 3–4 km up to 5–6 km

generally did not change the estimated smoke plume maximum height. The invariance of the estimated height within such an extended range of the $r_{max}$ can be considered as a criterion for validity of the estimated smoke-plume maximum height.

## 3. Summary

The maximum height of the smoke plume from biomass burning is one of the critical factors which determines the impact of fire emissions on air quality. To prescribe the vertical distribution of fire emissions, which are a critical input for the smoke-dispersion and air-quality models, proper plume rise models are required. While many plume rise models exist, their uncertainties, biases, and application limits when applied to biomass fires are not well characterized. The poor state of model evaluation in large part is mainly due to a lack of appropriate observational datasets.

Ground-based scanning lidar allows some addressing of this critical observation gap by obtaining important information on the levels and variations of the maximum smoke-plume heights in the smoke-polluted areas. The lidar data processing algorithms considered in the paper are based on the analysis of the intercept function, extracted directly from the recorded lidar signal, and the square-range-corrected backscatter signal normalized similarly to the above intercept function. The normalization of the square-range-corrected backscatter signal allows application of the same principles as those used in the analysis of the intercept function but allows obtaining additional characteristics of the smoke plume that can be used for improvement of smoke-dispersion and air-quality models.

### References

1. N. H. F. French, P. Goovaerts, and E. S. Kasischke, "Uncertainty in estimating carbon emissions from boreal forest fires," J. Geophys. Res. **109**, D14S08 (2004).
2. B. Langmann, B. Duncan, C. Textor, J. Trentmann, and G. R. van der Werf, "Vegetation fire emissions and their impact on air pollution and climate," Atmos. Environ. **43**, 107–116 (2009).
3. S. M. Raffuse, K. J. Craig, N. K. Larkin, T. T. Strand, D. C. Sullivan, N. J. M. Wheeler, and R. Solomon, "An evaluation of modeled plume injection height with satellite-derived observed plume height," Atmosphere **3**, 103–123 (2012).
4. R. J. Dirksen, K. F. Boersma, J. de Laat, P. Stammes, G. R. van der Werf, M. V. Martin, and H. M. Kelder, "An aerosol boomerang: rapid around-the-world transport of smoke from the December 2006 Australian forest fires observed from space," J. Geophys. Res. **114**, D21201 (2009).
5. V. Amiridis, E. Giannakaki, D. S. Balis, E. Gerasopoulos, I. Pytharoulis, P. Zanis, S. Kazadzis, D. Melas, and C. Zerefos, "Smoke injection heights from agricultural burning in Eastern Europe as seen by CALIPSO," Atmos. Chem. Phys. **10**, 11567–11576 (2010).
6. R. A. Kahn, Y. Chen, D. L. Nelson, F.-Y. Leung, Q. Li, D. J. Diner, and J. A. Logan, "Wildfire smoke injection heights: two perspectives from space," Geophys. Res. Lett. **35**, L04089 (2008).
7. A. J. Soja, T. D. Fairlie, D. J. Westberg, and G. Pouliot, "Biomass burning plume injection height using CALIOP, MODIS and the NASA Langley Trajectory Model," http://www.epa.gov/ttnchie1/conference/ei20/session7/asoja.pdf.
8. http://www.firescience.gov/projects/briefs/04-1-1-04_FSBrief103.pdf.
9. W. E. Heilman, Y. Liu, S. Urbanski, V. Kovalev, and R. Mickler, "Wildland fire emissions, carbon, and climate: plume rise, atmospheric transport, and chemistry processes," Forest Ecol. Manage. **317**, 70–79 (2014).
10. S. Luchs and J. Pendergrast, "Using dual polarimetric radar to assess prescribed and wildland fire intensity in Florida," in *Proceedings of 17th Conference on Integrated Observing and Assimilation Systems for the Atmosphere (a) European Microwave Conference (EuMC'12)*, (IEEE, 2012), pp. 1335–1338.
11. V. Kovalev, W. M. Hao, C. Wold, J. Newton, D. J. Latham, and A. Petkov, "Investigation of optical characteristics and smoke-plume dynamics in the wildfire vicinity with lidar," Proc. SPIE **7089**, 708906 (2008).
12. V. A. Kovalev, A. Petkov, C. Wold, S. Urbanski, and W. M. Hao, "Determination of smoke plume and layer heights using scanning lidar data," Appl. Opt. **48**, 5287–5294 (2009).
13. V. A. Kovalev, A. Petkov, C. Wold, and W. M. Hao, "Lidar monitoring of regions of intense backscatter with poorly defined boundaries," Appl. Opt. **50**, 103–109 (2011).
14. V. A. Kovalev, A. Petkov, C. Wold, S. Urbanski, and W. M. Hao, "Essentials of multiangle data-processing methodology for smoke polluted atmospheres," Rom. J. Phys. **56**, 520–529 (2011).
15. S. Urbanski, V. Kovalev, W. M. Hao, C. Wold, and A. Petkov, "Lidar and airborne investigation of smoke plume characteristics: Kootenai Creek Fire case study," in *Proceedings of the 25th International Laser Radar Conference*, St. Petersburg, Russia, July 5–9, 2010, pp. 1051–1054.